BMES BIOMEDICAL ENGINEERING Check for updates

Original Article

Chondroitin Sulfate Promotes Interstitial Cell Activation and Calcification in an *In Vitro* Model of the Aortic Valve

Sudip Dahal, ¹ Jonathan Alejandro Bramsen, ¹ Bridget R. Alber, ¹ Bruce T. Murray, ² Peter Huang, ² Mei-Hsiu Chen, ³ and Gretchen J. Mahler ¹

¹Department of Biomedical Engineering, Binghamton University, Binghamton, NY, USA; ²Department of Mechanical Engineering, Binghamton University, Binghamton, NY, USA; and ³Department of Mathematical Sciences, Binghamton University, Binghamton, NY, USA

(Received 15 June 2021; accepted 19 October 2021)

Associate Editor Igor Efimov oversaw the review of this article.

Abstract

Purpose—Calcific aortic valve disease (CAVD), has been characterized as a cascade of cellular changes leading to leaflet thickening and valvular calcification. In diseased aortic valves, glycosaminoglycans (GAGs) normally found in the valve spongiosa migrate to the collagen I-rich fibrosa layer near calcified nodules. Current treatments for CAVD are limited to valve replacement or drugs tailored to other cardiovascular diseases.

Methods—Porcine aortic valve interstitial cells and porcine aortic valve endothelial cells were seeded into collagen I hydrogels of varying initial stiffness or initial stiffness-matched collagen I hydrogels containing the glycosaminoglycans chondroitin sulfate (CS), hyaluronic acid (HA), or dermatan sulfate (DS). Assays were performed after 2 weeks in culture to determine cell gene expression, protein expression, protein secretion, and calcification. Multiple regression analyses were performed to determine the importance of initial hydrogel stiffness, GAGs, and the presence of endothelial cells on calcification, both with and without osteogenic medium.

Results—High initial stiffness hydrogels and osteogenic medium promoted calcification, while for DS or HA the presence of endothelial cells prevented calcification. CS was found to increase the expression of pro-calcific genes, increase activated myofibroblast protein expression, induce the secretion of collagen I by activated interstitial cells, and increase calcified nodule formation.

Conclusion—This study demonstrates a more complete model of aortic valve disease, including endothelial cells, interstitial cells, and a stiff and disease-like ECM. In vitro models of both healthy and diseased valves can be useful for

Address correspondence to Gretchen J. Mahler, Department of Biomedical Engineering, Binghamton University, Binghamton, NY, USA. Electronic mail: gmahler@binghamton.edu

Published online: 04 November 2021

understanding the mechanisms of CAVD pathogenesis and provide a model for testing novel therapeutics.

Keywords—Calcific aortic valve disease, Alpha smooth muscle actin, Glycosaminoglycan, Endothelial, Hyaluronic acid

INTRODUCTION

Calcific aortic valve disease (CAVD), which results in aortic valve stenosis, is the most common heart valve disease in the elderly, and the number of elderly patients with aortic valve stenosis is projected to more than double by 2050 in both the United States and Europe. Surgical valve replacement is currently the primary treatment for CAVD, as there is no effective pharmacological approach for slowing or preventing the progression of this disease. 16

The aortic valve is composed of three semilunar leaflets, which are further divided into three layers, the fibrosa, ventricularis, and spongiosa.⁵ The fibrosa is located on the aortic side of the leaflet and is composed largely of collagen I arranged in the circumferential direction, the spongiosa is the center layer composed primarily of glycosaminoglycans (GAGs), and the elastin-rich ventricularis forms the ventricular surface of the leaflet.^{5,41} Valve endothelial cells line all blood-contacting surfaces and are responsible for regulating permeability, inflammatory cell adhesion, and transmitting nutrient and biochemical signals to the interstitial cells.¹⁰ Valve interstitial cells are the primary cell type found in the three valve layers. Interstitial cells

organize, remodel, and produce extracellular matrix (ECM) proteins to maintain the valve matrix in response to dynamic tissue strains. ^{2,32,36}

Valve interstitial cells can become activated and differentiate into myofibroblast-like cells in response to the microenvironment, and can be identified by contractility markers such as α-smooth muscle actin (α-SMA). 40 Prolonged activation of the interstitial cells can result in valve ECM disruption, pathological interstitial cell differentiation towards osteoblast-like cells, which is associated with expression of the transcription factor RUNX2 and in later stages osteocalcin, and valve matrix calcification.³⁵ One additional source of myofibroblasts is endothelial to mesenchymal transformation or EndMT. EndMT is the change in phenotype of endothelial cells to mesenchymal-like cells, resulting in activated myofibroblasts that can secrete cytokines and remodel the ECM. EndMT was first observed in embryonic heart valve development^{22,23} and although the primary role of EndMT in adult physiology is unknown previous studies have demonstrated that EndMT is present in CAVD, 6,21 and EndMT is becoming recognized as a potential target in the treatment of cardiac pathology. 18

CAVD progresses from mild valve thickening (aortic sclerosis) to severe valve calcification (aortic stenosis). Early valve disease is characterized by deposition of the chondroitin sulfate (CS) and dermatan sulfate (DS)-rich proteoglycans biglycan and decorin into the sub-endothelial fibrosa layer, which is normally composed of collagen I, 27,28,38 while the latestage valve disease fibrosa displays the proteoglycans decorin, biglycan, versican, and the GAG hyaluronic acid (HA) near calcified aortic valve nodules. 9,13,14,39 In our previous work, an in vitro assay that mimics the detrimental ECM changes present in early and late calcific aortic valve disease was developed with 3D, collagen I and GAG (CS, HA, or DS) hybrid hydrogels and porcine aortic valve endothelial cells (PAVEC).6 Collagen-only stiffness controls made it possible to determine the individual contributions of stiffness and/or GAGs toward inducing EndMT. It was found that CS induced the highest rate of EndMT, as quantified by ACTA2 gene expression, a SMA protein expression, and matrix invasion; and led to the most collagen I and GAG production by mesenchymally transformed cells, indicating a cell phenotype most likely to promote fibrotic disease. Mesenchymal transformation induced by altered ECM was found to depend on cell-ECM bond strength and ERK1/2 signaling. Histological analysis of calcified human aortic heart valves demonstrated that GAGs were locally present near cells undergoing EndMT.⁶ In the current study, valve interstitial cells and osteogenic medium were incorporated into the previously described in vitro

model of early and later-stage valve disease. Standard assays in the field were performed after 2 weeks in culture to determine valve cell gene expression, protein expression, protein secretion, and calcification. Statistical analyses were carried out to first assess our primary hypothesis that GAGs increase calcification markers, as measured by $\alpha\text{-SMA}$ protein expression and Alizarin Red S (ARS) staining, in the model. Later, regression methods were used to evaluate our secondary hypothesis that increased initial hydrogel stiffness also induces calcifications; and that the presence of endothelial cells decreases calcification markers

MATERIALS AND METHODS

Cell Extraction and Culture

Porcine aortic valve endothelial cells (PAVEC) and porcine aortic valve interstitial cells (PAVIC) were used in the experiments. These cells were extracted from pig heart valves obtained from a local abattoir. Collagenase digestion protocols described by Butcher et al.^{3,4} were used to extract cells. PAVEC were grown in flasks coated with 50 μg/mL rat tail collagen I (BD[©] Biosciences, San Jose, CA). PAVEC and PAVIC were cultured at 37 °C and 5% CO₂ in DMEM supplemented with 10% FBS (Gemini Bio-Products Gem-CellTM, West Sacramento, CA), and 1% penicillinstreptomycin (Invitrogen, Carlsbad, CA). PAVEC medium was also supplemented with 50 U/mL heparin (Sigma-Aldrich, St. Louis, MO). Culture medium was changed every 48 h. PAVEC were passaged with 0.05% Trypsin-EDTA (ThermoFisher Scientific) 1:3 at confluence. PAVIC were passaged with 0.25% Trypsin-EDTA (Invitrogen) after reaching confluence. PAVIC and PAVEC were used between passages 3 and 5. Endothelial culture purity was confirmed via realtime PCR for α-smooth muscle actin (not expressed in PAVEC but expressed in PAVIC and in cells undergoing EndMT). Cultures with undetectable expression (cycle threshold > 37 cycles) were used in subsequent experiments.²¹

3D Gel Preparation

3D hydrogel preparation was previously described by Dahal et al. Briefly, collagen I gel solution was prepared by mixing ice-cold 3X, 5X or 10X Dulbecco's Modified Eagle's Medium (DMEM, Invitrogen), 10% FBS , sterile 18 M Ω water, 0.1 M NaOH, rat tail collagen type I, and PAVIC at a concentration of 1 \times 106 cells/mL. The concentration of collagen was varied to obtain 1.5, 2 or 2.2 mg/mL collagen in the gel. Gels



containing GAGs at a concentration of 1, 10, or 20 mg/mL were made with 1.5 mg/mL collagen. In our previous work we determined that collagen gels with a collagen concentration of 1.5 mg/mL collagen serve as a stiffness control for 1.5 mg/mL collagens + 1 mg/mL GAG gels (referred to as low hydrogel stiffness), 2.0 mg/mL collagen gels serve as a stiffness control for 1.5 mg/mL collagen + 10 mg/mL GAG gels (referred to as intermediate hydrogel stiffness), and 2.2 mg/mL collagen gels serve as stiffness controls for 1.5 mg/mL collagen + 20 mg/mL collagen gels (referred to as high hydrogel stiffness).⁶ The culture of PAVIC in the hydrogels for 14 days leads to compaction and remodeling of the ECM, which significantly alters the initial hydrogel stiffness. As demonstrated by Stevenson et al, the modulus is likely higher in the low starting collagen concentration hydrogels when compared with higher starting collagen concentration hydrogels due to greater compaction of low-concentration collagen gels.³⁷ Due to this change in hydrogel stiffness over time, the experimental conditions are referred to as low, medium, or high initial hydrogel stiffness.

GAGs used in the experiments were chondroitin sulfate (chondroitin sulfate A sodium salt from bovine trachea, Sigma-Aldrich), hyaluronic acid (hyaluronic acid sodium salt from Streptococcus equi, Sigma-Aldrich) and dermatan sulfate (chondroitin sulfate B sodium salt from porcine intestinal mucosa). Over 75% of GAGs are retained in the 3D collagen gel using this method. A volume of 300 μ L of the hydrogel solution containing 300,000 PAVIC was plated into 24-well tissue culture plates (1.9 cm² growth area; Corning, Corning, NY). After 1 h of incubation at 37 °C and 5% CO₂, the solution cross-linked and formed 3D hydrogel structures. Half of the hydrogels were used in PAVIC only experiments, while in half of the hydrogels PAVEC were then seeded on top of the hydrogels at a density of 5×10^5 cells/cm² (95,000 cells/well) in a volume of 0.3 mL culture medium. Cells were cultured for 14 days before further experiments were performed. Cells were cultured for 14 days to mimic previous relevant studies, which demonstrated significant calcific nodule formation while also maintaining cell viability in 14 day valve cell co-cultures. 15,33 Hydrogels were cultured in DMEM (control) or osteogenic medium (DMEM supplemented with 10 mmol/L β -glycerophosphate, 50 μ g/ mL ascorbic acid, and 10 nmol/L dexamethasone) with media changed every 48 h.

Immunocytochemistry

The hydrogels were washed with 1X phosphate buffered saline (PBS, Omnipur®, Baltimore, MD) and

fixed with 4% paraformaldehyde (Sigma-Aldrich, St. Louis, MO) overnight at 4 °C. Cells were then washed three times with PBS (15 min each on rotator) and permeabilized with 0.2% Triton X-100 (Sigma-Aldrich, 10 min on rotator). Next, cells were blocked with 1% BSA (RocklandTM, Limerick, PA) in PBS and incubated overnight at 4 °C. A 1:100 solution of primary antibody (rabbit anti-human α-SMA, Spring BioscienceTM, Pleasanton, CA) was added and incubated overnight at 4 °C. Next a 1:100 solution of secondary antibody (488 goat anti-rabbit, ThermoFisher Scientific) was added and incubated at room temperature for 2 h covered by aluminum foil. The samples were then washed three times with PBS (15 min each on rotator). A 1:1000 solution of DRAQ5 (ThermoFisher Scientific, Rockford, IL) far red DNA stain was then added and incubated for 30 min at room temperature. Finally, the gels were rinsed once with 18 $M\Omega$ water and stored in 18 $M\Omega$ water. The samples were then imaged using confocal microscope (Leica TCS SP5 Laser Scanning Confocal Microscope). The expression of α-SMA protein was quantified for each image using ImageJ and plotted as a percentage of 1.5 mg/mL collagen-only controls.³⁷

Gene Expression

RNA extraction and purification was performed using RNeasy® Mini Kit (Qiagen, Valencia, CA). DNA synthesis was carried out using iScriptTM cDNA Synthesis Kit (BioRad, Hercules, CA). Custom primers were obtained from ThermoFisher Scientific and were previously reported by Mahler et al. and Richards et al.^{21,33} Sequences are the following: 18S 5'-AATGGGGTTCAACGGGTTAC-3', forward: reverse: 5'-TAGAGGGACAAGTGGCGTTC-3'; ACTA2 $(\alpha$ -SMA) forward: 5'-CAGCCAG-GATGTGTGAAGAA-3', reverse: 5'-TCACCCCCT-GATGTCTAGGA-3'; Osteocalcin (BGLAP) forward: 5'-CTCCAGCCACAACATCCTTT-3', reverse: 5'-TGGCCTCCAGCACTGTTTAT-3'; RUNX2 forward: 5'-GCACTACCCAGCCACCTTTA-3', reverse: 5'-TATGGAGTGCTGCTGGTCTG-3'. RT-PCR was performed on all samples using SYBR Green PCR master mix (Applied Biosystems, Foster City, CA) and a MiniOpticon Real-Time PCR Detection System (Bio-Rad Laboratories, Hercules, CA). Gene expression was normalized to the expression of 18S and compared with 1.5 mg/mL collagen-only controls in regular medium using the $2^{-\Delta\Delta Ct}$ method.²⁰

Alizarin Red S Assay

Alizarin Red S (ARS) assays were carried out to quantify the calcium content of hydrogels. ARS is a



red stain that binds to calcium in cells or matrix fibers. The hydrogels were washed with 1X PBS and fixed with 4% paraformaldehyde overnight at 4 °C. Hydrogels were then washed three times with 1X PBS (5 min each on rotator) and then 500 μ L of 40 nmol/L ARS stain (Sigma-Aldrich) was added to each gel. Hydrogels were washed four times with 1X PBS (15 min each on rotator), and then rocked overnight in PBS to remove unbound stain. Bound ARS dye was then released from the hydrogels with 10% acetic acid, followed by neutralization with 10% ammonium hydroxide. The concentration of dye in solution was quantified with a plate reader (BioTek Synergy 2, Winooski, VT) at 405 nm.

Total DNA Quantification and Collagen and GAG Secretion Assays

Prior to the quantification of collagen, GAG and DNA in hydrogels, a papain digestion of the hydrogels containing cells was performed. First PBE buffer was prepared by adding 7.1 g of sodium phosphate dibasic (Na₂HPO₄, SigmaAldrich) and 1.6 g of ethylenediaminetetraacetic acid disodium salt (EDTA-Na₂ SigmaAldrich) to 500 mL of 18 M Ω water. The pH was then adjusted to 6.5 and the solution was passed through a 0.22 μ m filter. Next, 0.035 grams of L-cysteine was added to 20 mL of PBE buffer to make a 10 mM solution. The solution was filtered and 100 μ L of sterile papain enzyme solution (Sigma Aldrich) was added. Finally, papain enzyme solution was added to each 3D gel and incubated at 37 °C for 16 h. Following the completion of incubation, collagen, GAG and DNA quantification assays were performed on each gel.

A DNA assay kit (Chondrex, Redmond, WA) was used to quantify DNA to determine the proliferation of cells in PAVIC-only and PAVEC-PAVIC co-culture samples digested by papain. First, serial dilutions of the standard (calf thymus DNA standard) were prepared using the reaction solution from the kit. Next, 50 μ L of diluted standards or digested samples were added to respective wells of a 96-well plate. Then, 50 μ L of 1X detection solution was added to all the wells and the plate was incubated at room temperature for 5 min. Finally, the plate was read using a plate reader at excitation 360 nm/emission 460 nm. The standard curve for DNA quantification was used to quantify the DNA content in each sample.

A hydroxyproline assay kit (Chondrex, Redmond, WA) was used to quantify collagen secretion in PA-VIC-only or PAVEC-PAVIC co-culture samples digested by papain. First, standard dilutions were prepared by the serial dilutions of the standard with water. Next, chloramine T solution was prepared by

mixing 10 μ L of 10X chloramine T solution and 90 μ L of solution A (chloramine T dilution buffer) for each well. Then, 10 μ L of standards, distilled water (blanks) and digested samples were added into the appropriate wells of a 96-well plate. After that 100 μL of the 1X chloramine T solution was added to all the wells and the plate was incubated at room temperature for 20 min. Next, 1X dimethylaminobenzaldehyde (DMAB) solution was prepared by mixing 50 μL of 2X DMAB solution and 50 µL of solution B (DMAB dilution buffer) for each well. Then, 100 μ L of this 1X DMAB solution was added to all the wells followed by shaking of the well plate and incubation at 60 °C for 30 min. Finally, the absorbance was read at 550 nm using a plate reader. The standard curve for collagen quantification was used to quantify the hydroxyproline level (13.5% of the total collagen) followed by the quantification of collagen content in each sample. The content of collagen was normalized to controls and to the DNA content of the sample.

A glycosaminoglycan assay kit (Chondrex, Redmond, WA) was used to quantify sulfated GAG secretion in our PAVIC-only culture and PAVEC-PAVIC co-culture samples digested by papain. For the GAG quantification assay, serial dilutions of the standard (chondroitin-6-sulfate) were prepared by diluting with PBS. Next, 100 µL of standards, PBS (blanks) and digested samples were added into the appropriate wells of a 96-well plate. After that 100 μ L of 1,9 dimethylmethylene blue (DMB) dye solution was added to each well and 100 μL of PBS was added to the control wells. Finally, the absorbances were read at 530 nm using a plate reader. The standard curve for GAG quantification was used to quantify GAG content in each sample. The content of GAG was normalized to controls and to the DNA content of the sample.

Data Processing and Statistical Analysis

For gene expression data, separate Box-Cox transformations were carried out for each gene before linear regressions models were fitted using combinations of conditions. Conditions identified by the regression analysis as significant predictors were double-checked using Kruskal-Wallis tests, and/or Mann-Whitney tests. Log-transformed gene expression data from all replicates for each gene were further analyzed using hierarchical clustering with heatmap displays for all conditions to identify the relationship among the three genes under all possible combinations of conditions.

For the expression of α -SMA protein, univariable and multivariable regression models were fitted for combinations of important conditions. Experimental conditions of interest were cell type (PAVIC-PAVEC



co-culture or PAVIC), medium use (regular control medium or osteogenic medium), GAG (CS, DS, HA, or none) at three (low, intermediate and high) levels of initial hydrogel stiffness. The model with the largest variations explained was selected as the final model. Variables or interactions are considered statistically significant when P values are < 0.05.

Natural logarithm transformed DNA weight data in $\mu g/mL$ were fitted using linear regression models. The most parsimonious model with highest adjusted R^2 was selected as the final model. Similarly, positive collagen weight data (normalized to DNA weight) were analyzed using linear regression analysis, and natural logarithm transformed GAG weights (normalized to DNA weights) were also fitted using linear regression analyses. In addition, correlation between DNA weight and GAG weight were explored using Spearman's correlation.

For ARS stain (absorbance) data, the number of replicates available were very imbalanced depending on whether experiments were carried out for PAVIC only or PAVIC-PAVEC co-culture. Hence, separate analyses were first carried out for experiments with PAVIC only and co-cultures respectively to investigate predictive factors separately. The data were then combined to explore the common factors and their interactions with cell type on ARS stain. Data were analyzed using R: A language and environment for statistical computing, version 4.0.2, with packages lme4, MASS, gplots and RColorBrewer.

RESULTS

Gene Expression

For the genes ACTA2, RUNX2, and Osteocalcin there were a total of 48 unique experimental conditions with 2 to 5 replicates available for each condition. There were 180, 183, and 182 experimental data points from ACTA2, RUNX2, and Osteocalcin, respectively, available for analysis. Figure 1 displays the heatmap of natural logarithm transformed gene expression data from all available replicates of each condition. As shown in Figure 1, the RUNX2 was similar to Osteocalcin with PAVIC alone (left and right upper blocks) regardless of medium, GAG or initial hydrogel stiffness. However, RUNX2 was more similar to Osteocalcin for PAVIC-PAVEC co-culture in regular control medium (left lower block) for CS only regardless of initial hydrogel stiffness. For other GAGs, RUNX2 was more similar to ACTA2 (left lower block). For co-culture in osteogenic medium (right lower block), the RUNX2 exhibited patterns between ACTA2 and Osteocalcin.

Regression analysis and nonparametric tests (Kruskal-Wallis and Mann-Whitney tests) confirmed what we observed in Figure 1. Specifically, for ACTA2, compared to PAVIC alone (the first 5 columns in the top blocks), co-culture (the first 5 columns in the lower blocks) significantly suppressed expressions as the level of initial hydrogel stiffness increased and level of suppression depended on the type of GAG used, with DS and HA having similar patterns.

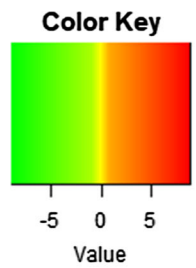
For RUNX2, compared to regular control medium (middle 5 columns in the left blocks), osteogenic medium (middle 5 columns in the right blocks) significantly increased expressions. The impacts of coculture versus PAVIC alone on RUNX2 expressions depended on the initial hydrogel stiffness and GAGs.

For Osteocalcin, similar to RUNX2, compared to regular control medium (last 5 columns in the left blocks), osteogenic medium (last 5 columns in the right blocks) significantly increased expressions. The impact of co-culture versus PAVIC alone on Osteocalcin expressions also depended on the initial hydrogel stiffness and GAGs, but the impact was strongest at the high initial hydrogel stiffness.

α-SMA Protein Expression

For expressions of α -SMA protein, 12 replicates were carried out for each of the unique experimental conditions for a total of 576 data points. The boxplots of α-SMA stained area (% of control) for every condition separately are displayed in Figure 2 and the Analysis of Variance table examining the significance of variables and their interactions are displayed in Table 1. For PAVIC alone (upper plots), α-SMA stained area increased as the initial hydrogel stiffness increased and the effects were significant (P < 0.001, Table 1). For PAVIC-PAVEC co-culture (lower plots), the effects of initial hydrogel stiffness on α -SMA stained area were not consistent. Use of osteogenic medium (right plots) increased the α-SMA expression when compared to the regular control medium (left plots). While PAVIC-PAVEC co-culture (lower plots) decreased the α-SMA stained area when compared to PAVIC alone (upper plots) at low initial hydrogel stiffness with no GAGs. However, the magnitudes depended on the initial hydrogel stiffness levels and which GAG was used (Table 1). Overall, the added GAG increased α -SMA stained area at similar proportions regardless of the initial hydrogel stiffness, but there were significant interaction effects between GAG and cell type (P < 0.001, Table 1).





log(Gene Expressions)

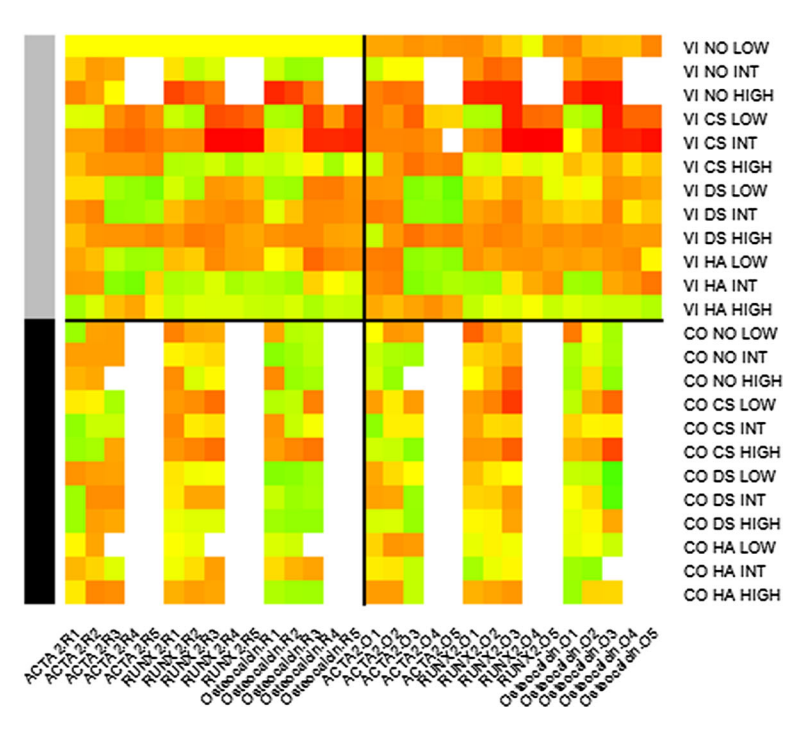


FIGURE 1. Heatmap for the log(gene expression) data for all three genes for each condition. Each column refers to the expression from one replicate under different experimental conditions. The left half refers to expressions with regular control medium, the right half refers to expressions with osteogenic medium. Row names: *CO* co-culture, *VI* PAVIC only, *NO* no GAGs. *LOW* low initial hydrogel stiffness, *INT* intermediate initial hydrogel stiffness, *HIGH* high initial hydrogel stiffness.

DNA

A total of 144 experimental data points were generated (3 replicates each for 48 experimental conditions). The results of DNA weights analysis are displayed in Table 2 and Figure 3. Univariable analysis indicated that PAVIC-PAVEC co-culture (lower plots) increased the log(DNA weights) when compared to PAVIC alone. Use of osteogenic medium decreased DNA weights when compared to control medium. Increase in initial hydrogel stiffness increased the DNA weights without GAG, and the effects of initial hydrogel stiffness might depend on the GAG and cell types. The addition of different GAG has different effects on DNA weights when compared to conditions where no GAG was added, and the effects were dependent on the initial hydrogel stiffness. Hence, a multivariable regression model was selected with GAG type (CS, DS, and HA in reference to none), initial hydrogel stiffness (low, intermediate and high with low

stiffness as reference), indicators for co-culture (with PAVIC only as reference), and osteogenic medium (control medium as reference) as main effects, along with their interaction effects. Consistent with our univariable analysis, osteogenic medium (P=0.01) significantly decreased the DNA weights in comparison to control medium, while the PAVIC-PAVEC coculture significantly increased the DNA weights when compared to PAVIC alone (P<0.001), and there were significant interaction effects of cell type and initial hydrogel stiffness. Furthermore, the initial hydrogel stiffness also exhibited different effects for different GAGs.

Collagen Secretion

Collagen weights remained positive when CS was added at high initial hydrogel stiffness after normalizing by DNA weights. Four boxplots of Collagen



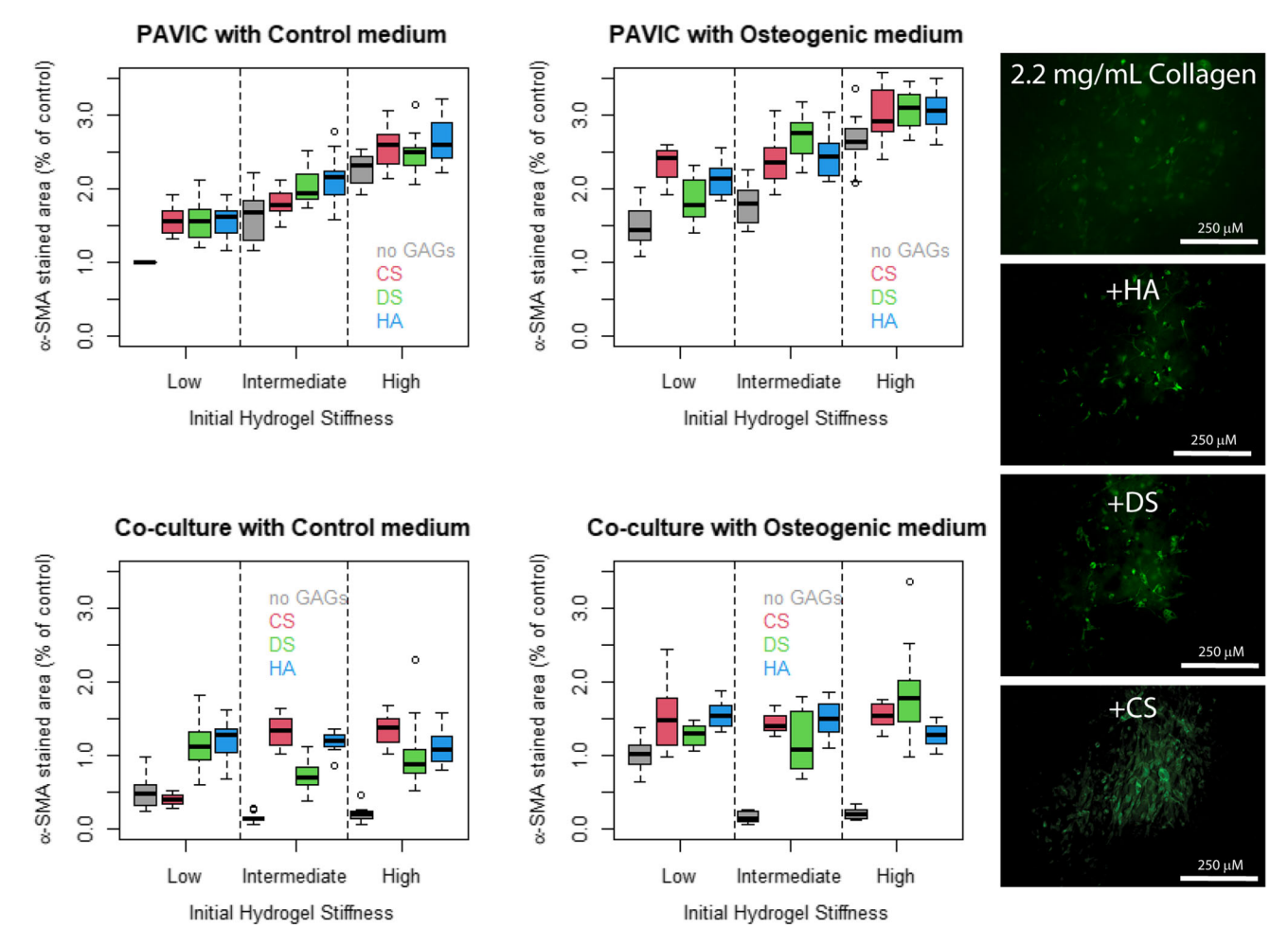


FIGURE 2. Boxplots of α -SMA protein stained area (% of control) values for combinations of GAG and initial hydrogel stiffness, separately for PAVIC and co-culture of PAVIC-PAVEC with either regular control or osteogenic medium. In each of the subplot: Grey: no GAGs, Red: CS, Green: DS, Blue: HA. In each boxplot, the middle box marks the first quartile to the 3rd quartile, with a line marking the median. The whiskers extend to the lowest and highest values, with the exceptions of outliers which are marked by circles. Right: representative images for co-cultures in control medium with high initial hydrogel stiffness and high GAG content.

TABLE 1. Analysis of variance (ANOVA) table of expression of α -SMA protein stained area (% of control) and the important predictors.

Parameter	Df	Sum of squared errors	Mean Squared errors	F value	P value
Medium (regular or osteogenic)	1	24.71	24.71	220.73	< 0.001
Cell type (PAVIC or co-culture)	1	184.98	184.98	1652.16	< 0.001
GAG (CS, DS, HA or none)	3	52.17	17.39	155.33	< 0.001
Initial hydrogel stiffness (low, intermediate, high)	2	26.77	13.39	119.57	< 0.001
Cell type and GAG interactions	3	4.18	1.39	12.43	< 0.001
Cell type and IHS interactions	2	26.6	13.3	118.8	< 0.001
Residuals	563	63.03	0.11		

A P value < 0.05 indicates the effect for that variable or interaction is statistically significant. IHS initial hydrogel stiffness.

weight/DNA weight were presented in Figure 4 for combinations of cell type (PAVIC alone or co-culture) and medium used (regular control or osteogenic medium). For PAVIC alone (left side), the use of osteogenic medium (green boxplot) increased the normalized collagen weight compared to regular con-

trol medium (red boxplot). On the other hand, for coculture (right side), the use of osteogenic medium (green boxplot) decreased the normalized collagen weight compared to regular control medium (red boxplot).



TABLE 2. ANOVA table for log(DNA weights) and the important predictors.

Parameter	Df	Sum of squared errors	Mean Squared errors	F value	P value
Medium (regular or osteogenic)	1	1.37	1.37	6.35	0.01
Cell type (PAVIC or co-culture)	1	1.95	1.95	9	< 0.001
GAG (CS, DS, HA or none)	3	8.9	2.97	13.72	< 0.001
Initial hydrogel stiffness (low, intermediate, or high)	2	9.19	4.59	21.24	< 0.001
Cell type and IHS interactions	2	2.43	1.21	5.61	< 0.001
GAG and IHS interactions	6	14.53	2.42	11.2	< 0.001
Residuals	128	27.69	0.22		

A P value < 0.05 indicates the effect for that variable or interaction is statistically significant. IHS initial hydrogel stiffness.

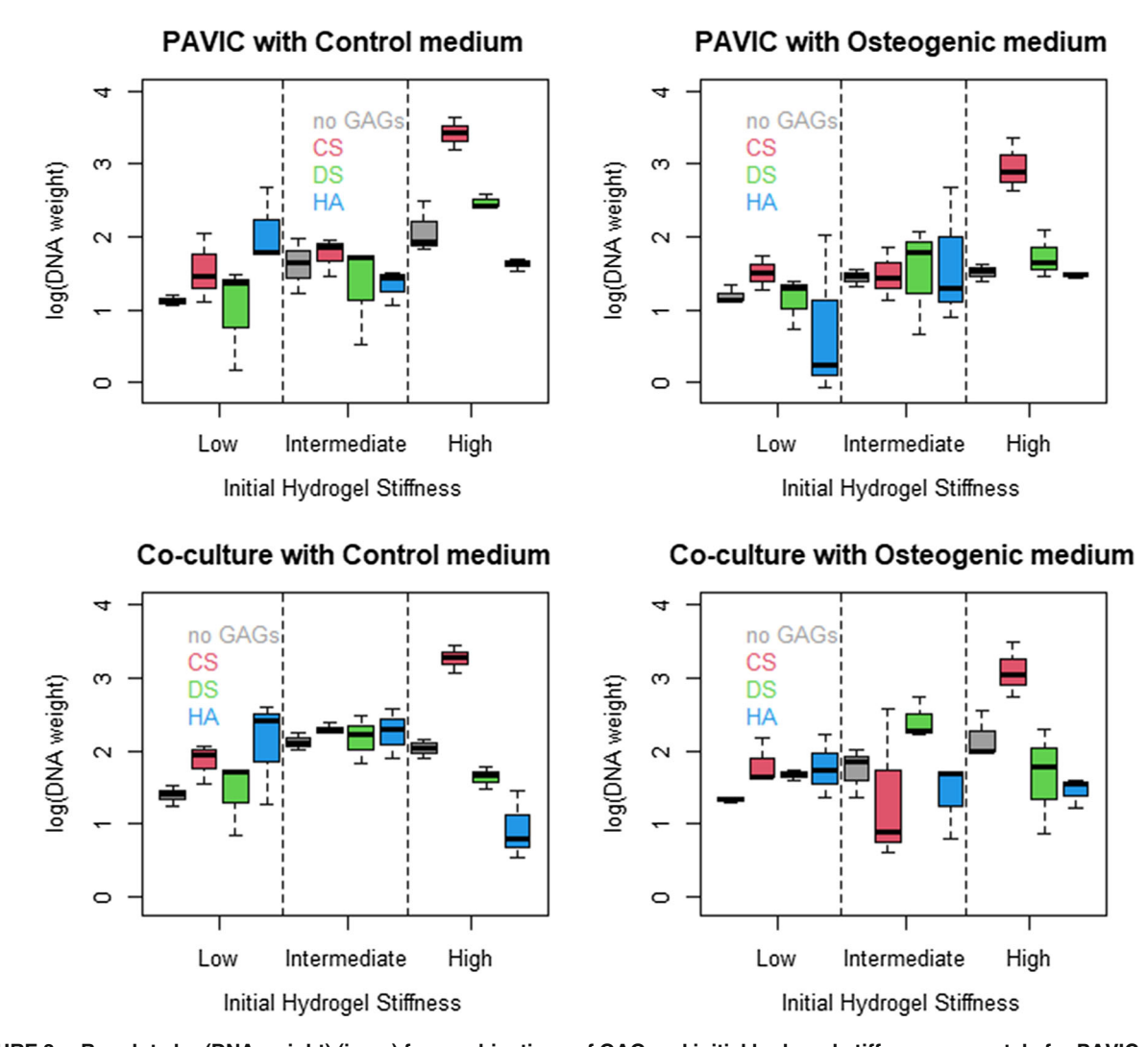


FIGURE 3. Boxplots log(DNA weight) (in μ g) for combinations of GAG and initial hydrogel stiffness, separately for PAVIC and coculture of PAVIC-PAVEC with either control or osteogenic medium. In each of the subplots: Grey: no GAGs, Red: CS, Green: DS, Blue: HA. In each boxplot, the middle box marks the first quartile to the 3rd quartile, with a line marking the median. The whiskers extend to the lowest and highest values, with the exceptions of outliers which are marked by circles.

GAG Secretion

After adjusting for DNA weights and being logtransformed, there is an outlier among the GAG secretion data. As a result, the data were analyzed with and without the outlier and there was no significant effect on the final model due to the outlier. Hence, the results were presented excluding the outlier. Univariate analyses show that there was no consistent effect of different initial hydrogel stiffness levels on the log (GAG/DNA). PAVIC-PAVEC co-culture tended to



increase the log(GAG/DNA) when compared to PA-VIC alone. The only effect from different GAG types was from DS and there was no consistent initial hydrogel stiffness effect. Hence, multivariate regression models were fitted and a final model with indicators for co-culture and osteogenic medium along with their interactions were included. In addition, indicators for different GAG were added to measure their effects on log(GAG/DNA) controlling for media and cell type. Table 3 and Figure 5 show the results for the ANOVA table of the final model excluding the one outlier. There was no significant difference among different initial hydrogel stiffness levels on log(GAG/DNA). The added DS GAG significantly decreased the log(GAG/DNA) compared to no GAGs, but the results were not consistent for other GAGs. For both media, the PAVIC-PAVEC co-culture (lower plots) increased

CS GAG at High Initial Hydrogel Stiffness

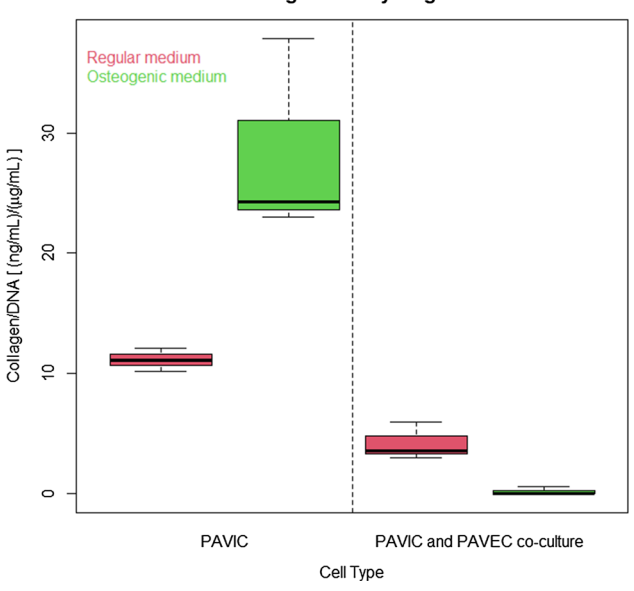


FIGURE 4. Normalized collagen weights (after being standardized against DNA) for conditions with the GAG CS and high initial hydrogel stiffness. The red color is for regular control medium, while green color is for osteogenic medium. In each boxplot, the middle box marks the first quartile to the 3rd quartile, with a line marking the median. The whiskers extend to the lowest and highest values, with the exceptions of outliers which are marked by circles.

the log(GAG/DNA) when compared to PAVIC alone (upper plots), and the magnitude was larger for regular control medium (left plots). For PAVIC alone, the osteogenic medium (right upper plot) increased the log(GAG/DNA) when compared to regular control medium (left upper plot). However, for PAVIC-PAVEC co-culture, the osteogenic medium (right lower plot) decreased log (GAG/DNA) when compared to regular medium (left lower plot). However, there is still a great deal of variation that cannot be explained by the model. There was a mild negative correlation between log(DNA weight) and log(GAG weight), with larger log(DNA weight) generally corresponding to smaller value of log(GAG weight). The Spearman correlation is estimated to be -0.36 with 95% confidence interval estimated to be (-0.50, -0.20).

Alizarin Red Stain Extraction and Quantification

Boxplots of ARS stain area are shown in Figure 6 and the ANOVA table of the analysis is in Table 4. For both cell type (PAVIC only or co-culture), osteogenic medium (right plots) increased the ARS stain area when compared to regular control medium (left plots) overall, but the magnitudes depended on the initial hydrogel stiffness level. Furthermore, the levels of ARS stain area depended on the interactions of GAG, Cell type, medium used and initial hydrogel stiffness.

DISCUSSION

This study investigated the individual contributions of initial 3D ECM (hydrogel) stiffness, GAGs, endothelial cells/EndMT, and osteogenic medium toward calcification in an *in vitro* model of the aortic valve. This study was motivated by previous findings indicating that chondroitin sulfate increases EndMT in a valve and tumor model, 6,25 and a lack of understanding of the potential role of EndMT in valvular pathogenesis. Although surgical treatments for aortic stenosis exist, there are still no effective pharmacological therapies that can slow or halt aortic valve disease progression. A physiologically realistic model of valve disease would help to reveal the

TABLE 3. ANOVA table for log(GAG/DNA) and the important predictors.

Parameter	Df	Sum of squared errors	Mean Squared errors	F value	P value	
Medium (regular or osteogenic	1	0.02	0.02	0.02	0.88	
Cell type (PAVIC or co-culture)	1	13.02	13.02	15.41	< 0.001	
GAG (CS, DS, HA or none)	3	5.75	1.92	2.27	0.08	
Medium and cell type interactions	1	3.66	3.66	4.33	0.04	
Residuals	136	114.94	0.85			

A P value < 0.05 indicates the effect for that variable or interaction is statistically significant.



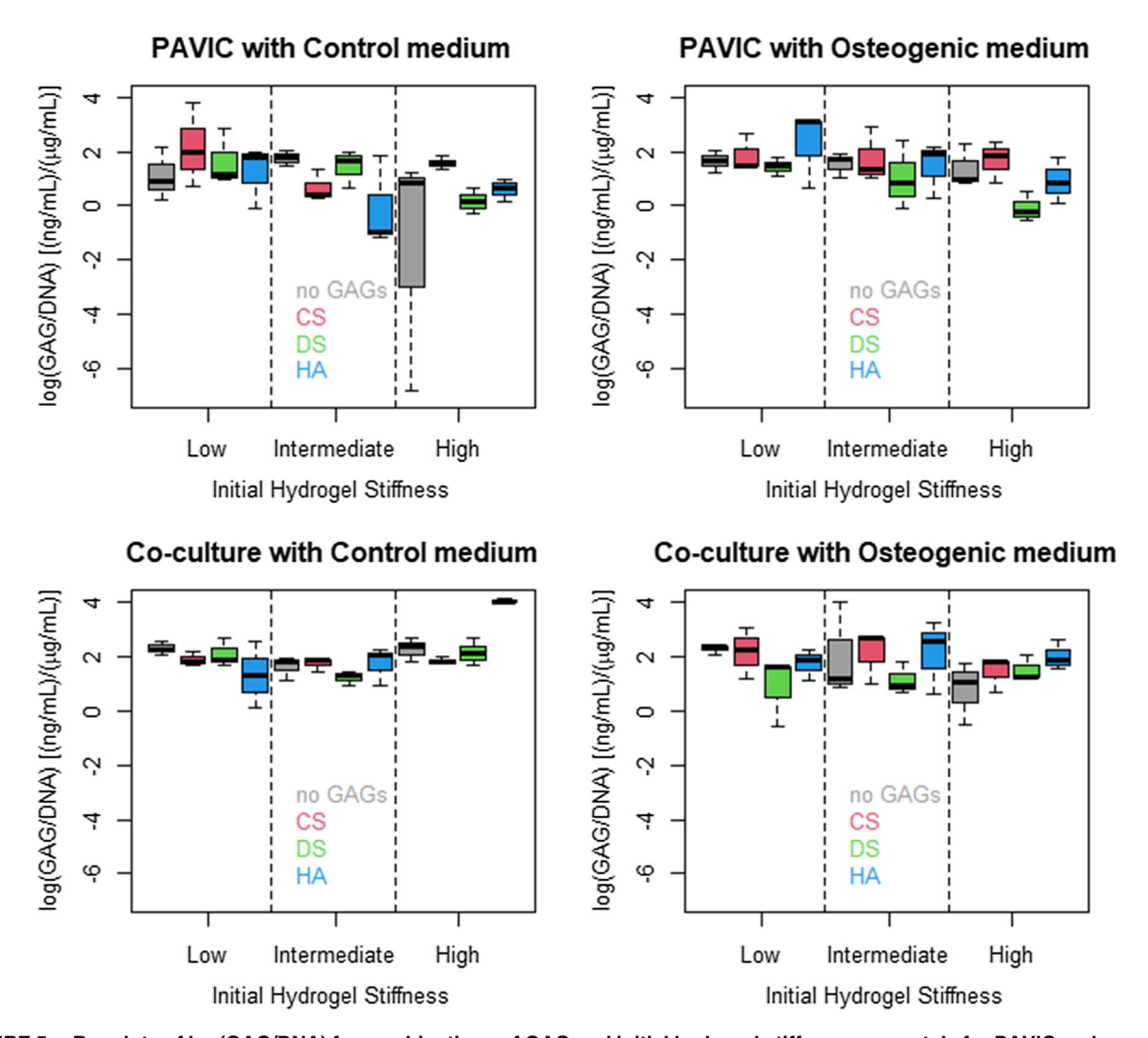


FIGURE 5. Boxplots of log(GAG/DNA) for combinations of GAG and initial hydrogel stiffness, separately for PAVIC and co-culture of PAVIC-PAVEC with either regular control or osteogenic medium. In each of the subplots: Grey: no GAGs, Red: CS, Green: DS, Blue: HA. In each boxplot, the middle box marks the first quartile to the 3rd quartile, with a line marking the median. The whiskers extend to the lowest and highest values, with the exceptions of outliers which are marked by circles.

mechanisms underlying valve calcification, and could possibly lead to new biomarkers or drug targets.

Addition of osteogenic culture medium to *in vitro* valve models is expected to increase pro-osteogenic differentiation and calcification. In the current study, osteogenic medium increased the expression of pro-osteogenic genes, α-SMA protein expression, GAG secretion, and calcification, and decreased cell proliferation as measured via total culture DNA content. These results agree with previous 3D models of the aortic valve with both porcine and human cells.^{7,33} Osteogenic medium was used in this study as a positive control to initiate calcific nodule formation in the model. The addition of GAGs to the ECM and increased initial hydrogel stiffness in the absence of osteogenic medium, however, were able to significantly increase α-SMA expression, cell proliferation, collagen

secretion, and calcific nodule formation. Primary fibroblasts isolated from cardiac tissue are difficult to maintain in culture in a quiescent phenotype due to their phenotype plasticity and mechanical sensitivity. Previous work by Landry et al. has shown that rat and mouse primary cardiac fibroblasts can be isolated and maintained for a longer period (3 days) in a quiescent state by decreasing the stiffness of the culture hydrogel and limiting the nutrient content of the cell culture medium to 2% serum. Phe control medium used in the current study contained 10% serum, and this alone may have contributed to valve cell differentiation toward myofibroblasts.

Activated interstitial (ACTA2) and osteoblast-like differentiation (Osteocalcin) gene expression were significantly decreased in cultures containing both interstitial and endothelial cells as initial hydrogel stiffness



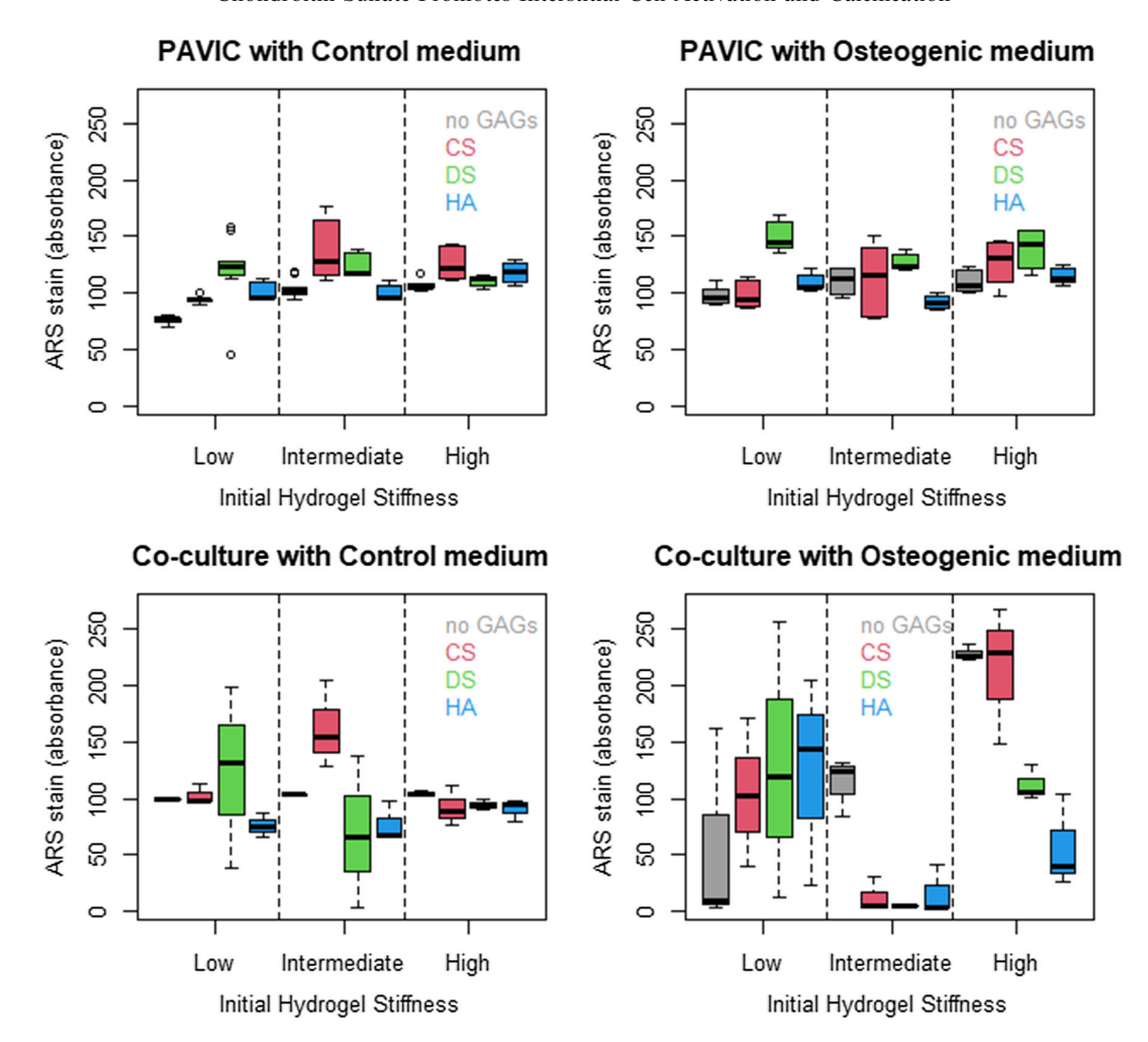


FIGURE 6. Boxplots of ARS dye values for combinations of GAG and initial hydrogel stiffness, separately for PAVIC and coculture of PAVIC-PAVEC with either Control or Osteogenic medium. In each of the subplots: Grey: no GAGs, Red: CS, Green: DS, Blue: HA. In each boxplot, the middle box marks the first quartile to the 3rd quartile, with a line marking the median. The whiskers extend to the lowest and highest values, with the exceptions of outliers, which are marked by circles.

TABLE 4. ANOVA table for ARS Stain data with dye extractions and quantifications.

Parameter	Df	Sum of squared errors	Mean Squared errors	F value	P value
GAG (CS, DS, HA or none)	3	19603.68	6534.56	6.79	< 0.001
Initial hydrogel stiffness (low, intermediate, high)	2	17523.73	8761.86	9.1	< 0.001
Cell type (PAVIC or co-culture)	1	10187.76	10187.76	10.58	< 0.001
Medium (regular or osteogenic)	1	1198.56	1198.56	1.24	0.27
GAG and cell type interactions	3	28678.64	9559.55	9.93	< 0.001
IHS and cell type interactions	2	24251.72	12125.86	12.59	< 0.001
IHS and medium interactions	2	22605.26	11302.63	11.74	< 0.001
GAG and IHS interactions	6	31460	5243.33	5.45	< 0.001
Residuals	267	257107	962.95		

A P value < 0.05 indicates the variable or interaction term is statistically significant. IHS initial hydrogel stiffness.

increases without GAG. Co-culture of PAVIC and PAVEC also decreased the protein expression of α -SMA, a myofibroblast differentiation marker, as initial hydrogel stiffness increases without GAG. The rela-

tionship between co-culture of PAVIC and PAVEC and calcification as measured with ARS depends on combinations of multiple factors. When GAGs were added, PAVEC generally decreased calcification,



except in high initial hydrogel stiffness and +CS conditions. These results are supported by previous results from Richards et al., demonstrating that valve endothelial nitric oxide signaling inhibited interstitial cell osteogenic differentiation.³³ These results also suggest that conditions leading to enhanced EndMT may accelerate calcification.6 Co-culture of PAVIC and PAVEC led to an increase in GAG secretion from the valve model, indicating that the presence of mesenchymally transformed endothelial cells could lead to changes in matrix secretion by the interstitial cells and/ or transformed endothelial cells. The culture system used in the current study prevented the use of methods described by Dahal et al. for quantifying EndMT, and therefore PAVIC-only cultures were used as an EndMT-null control. Gee et al. have recently developed a model using a constrained collagen gel coupled with a Boyden chamber to better isolate the role of EndMT on calcific lesion formation. 11 In this system both direct and indirect culture of PAVIC and PAVEC in osteogenic medium resulted in calcific deposition and pro-endochondral programming, PAVEC EndMT underwent and populated the center of calcified lesions, and calcification was exacerbated by the presence of endothelial cells, similar to results in the current study with co-culture in high initial stiffness and +CS conditions. 11

PAVIC only cells cultured within high initial hydrogel stiffness gels (2.2 mg/mL collagen) showed a significant upregulation in RUNX2 and Osteocalcin gene expression, indicating a differentiation toward osteoblast-like cells. Initially stiffer hydrogels also showed significant increases in α-SMA expression, increased cell proliferation as measured by DNA content in the gels, and an increase in calcification over low initial stiffness collagen controls for PAVIC-only. Previous work has shown that stiffened substrates initiate a myofibroblastic phenotype in valve interstitial cells. 17,31 3D hydrogels with tunable matrix stiffness developed by Duan et al. showed greater osteoblast differentiation in hydrogels with lower initial stiffness than valve leaflet layers, and suggested that ECM disruption, such as infiltration of proteoglycans into the valve fibrosa resulting in local tissue stiffness decreases, can promote CAVD progression. Duan et al. also used human cells, and did not include endothelial cells in their model, however.

ECM composition has previously been shown to influence valve interstitial cell differentiation and the production of native extracellular matrix ECM within *in vitro* models. 12,24,34 In the current study, the addition of chondroitin sulfate showed the most dramatic and clear results. The addition of CS to hydrogels upregulated ACTA2, RUNX2, and Osteocalcin expression, increased α -SMA expression, increased proliferation,

induced the secretion of collagen, and increased calcification for both PAVIC only cultures and co-cultures. In previous work CS contributed to ECM secretion and endothelial transformation and migration in a tumor model.²⁶ Tumor-associated changes in the stroma of human malignant lesions often include a significant increase in CS content, which can modify tumor metastasis due to the increased binding potential of these disaccharides.³⁰ Previous work with collagen-CS hydrogels and PAVIC showed that CS-rich hydrogels significantly increased EndMT, mesenchymally transformed cell invasion into the matrix, and collagen I and GAG production by the mesenchymally transformed cells.⁶ Results from the current study demonstrate that CS-rich hydrogels can induce calcification even in the absence of osteogenic medium. Collagen secretion (indicating a pro-fibrotic disease environment) is measurable only in the highest concentration CS hydrogels, with PAVIC-only cultures in osteogenic medium showing the highest levels of collagen secretion and co-cultures in control medium showing increased collagen secretion compared with co-cultures in osteogenic medium. These results show that, in an in vitro model, endothelial cells mediate valve disease progression, but cannot overcome the pathogenic signaling initiated by CS.

CONCLUSIONS

In conclusion, this study describes an in vitro model of the healthy and diseased aortic valve. PAVIC and PAVEC were seeded into 3D, collagen type 1 hydrogels of varying initial stiffness or initial stiffness-matched collagen I gels containing GAGs. Cellular progression toward myofibroblasts and/or osteoblastlike cells, ECM secretion, and calcification were measured after 2 weeks in culture. Statistical modeling of the data showed that high collagen I concentration hydrogels and osteogenic medium promoted osteoblast-like differentiation and calcification, while the presence of endothelial cells slowed disease progression in the tissue model. Chondroitin sulfate was found to increase pro-myofibroblast and pro-osteoblast differentiation gene expression, enhance myofibroblast protein expression, increase the secretion of collagen I by activated interstitial cells, and increase the formation of calcified nodules even in the absence of osteogenic medium. This study shows that a more complete model of aortic valve disease, including endothelial cells, interstitial cells, and a stiffened and disease-like ECM can provide a better environment for understanding valve disease pathogenesis and potentially finding new disease targets.



ACKNOWLEDGMENTS

We would like to thank Owasco Meat Company, Moravia, NY and The Boy's Meat Plant, Montrose, PA for providing porcine tissue samples.

AUTHOR CONTRIBUTION

GM, BM, PH, and MC contributed to conception and design of the study. SD, JB, and BA conducted experiments. MC performed the statistical analysis. SD wrote the first draft of the manuscript. GM, BM, PH, and MC edited the manuscript. All authors contributed to manuscript revision, read, and approved the submitted version.

FUNDING

This work was supported by the National Science Foundation (grant numbers CMMI 1436173, CMMI 1919438) and the Binghamton University Clifford D. Clark Diversity Fellowship for Graduate Students (JB).

DATA AVAILABILITY

All data and materials will be made available upon request.

CODE AVAILABILITY

Not applicable

CONFLICT OF INTEREST

The authors declare that the research was conducted in the absence of any commercial or financial relationships that could be construed as a potential conflict of interest.

ETHICS APPROVAL

Not applicable

CONSENT TO PARTICIPATE

Not applicable

CONSENT FOR PUBLICATION

Not applicable

REFERENCES

- ¹Benjamin, E. J., P. Muntner, A. Alonso, M. S. Bittencourt, C. W. Callaway, A. P. Carson, et al. Heart disease and stroke statistics-2019 update: a report from the American Heart Association. *Circulation*. 139(10):e56–e528, 2019. h ttps://doi.org/10.1161/cir.00000000000000659.
- ²Butcher, J. T., and R. M. Nerem. Porcine aortic valve interstitial cells in three-dimensional culture: comparison of phenotype with aortic smooth muscle cells. *J. Heart Valve Dis.* 13(3):478–485, 2004.
- ³Butcher, J. T., and R. M. Nerem. Valvular endothelial cells regulate the phenotype of interstitial cells in co-culture: effects of steady shear stress. *Tissue Eng.* 12(4):905–915, 2006.
- ⁴Butcher, J. T., A. M. Penrod, A. J. Garcia, and R. M. Nerem. Unique morphology and focal adhesion development of valvular endothelial cells in static and fluid flow environments. *Arterioscler. Thromb. Vasc. Biol.* 24(8):1429–1434, 2004. https://doi.org/10.1161/01.ATV.00 00130462.50769.5a.
- ⁵Christie, G. W. Anatomy of aortic heart valve leaflets: the influence of glutaraldehyde fixation on function. *Eur. J. Cardio-Thorac. Surg.* 6(Suppl 1):S25–S32, 1992. (discussion S3)
- ⁶Dahal, S., P. Huang, B. T. Murray, and G. J. Mahler. Endothelial to mesenchymal transformation is induced by altered extracellular matrix in aortic valve endothelial cells. *J. Biomed. Mater. Res. A.* 105(10):2729–2741, 2017. https://doi.org/10.1002/jbm.a.36133.
- ⁷Duan, B., Z. Yin, L. Hockaday Kang, R. L. Magin, and J. T. Butcher. Active tissue stiffness modulation controls valve interstitial cell phenotype and osteogenic potential in 3D culture. *Acta Biomater*. 36:42–54, 2016. https://doi.org/10.1016/j.actbio.2016.03.007.
- ⁸Flanagan, T. C., B. Wilkins, A. Black, S. Jockenhoevel, T. J. Smith, and A. S. Pandit. A collagen-glycosaminoglycan co-culture model for heart valve tissue engineering applications. *Biomaterials*. 27(10):2233–2246, 2006. https://doi.org/10.1016/j.biomaterials.2005.10.031.
- ⁹Fondard, O., D. Detaint, B. Iung, C. Choqueux, H. Adle-Biassette, M. Jarraya, et al. Extracellular matrix remodelling in human aortic valve disease: the role of matrix metalloproteinases and their tissue inhibitors. *Eur. Heart J.* 26(13):1333–1341, 2005. https://doi.org/10.1093/eurheartj/ehi248.
- ¹⁰Frater, R. W., G. Gong, D. Hoffman, and K. Liao. Endothelial covering of biological artificial heart valves. *Ann. Thorac. Surg.* 53(3):371–372, 1992. https://doi.org/10.1016/0003-4975(92)90252-y.
- ¹¹Gee, T. W., J. M. Richards, A. Mahmut, and J. T. Butcher. Valve endothelial-interstitial interactions drive emergent complex calcific lesion formation in vitro. *Biomaterials*. 269:120669, 2021. https://doi.org/10.1016/j.biomaterials.20 21.120669.
- ¹²Gu, X., and K. S. Masters. Regulation of valvular interstitial cell calcification by adhesive peptide sequences. *J. Biomed. Mater. Res. A.* 93(4):1620–1630, 2010. https://doi.org/10.1002/jbm.a.32660.
- ¹³Hinton, R. B., Jr., J. Lincoln, G. H. Deutsch, H. Osinska, P. B. Manning, D. W. Benson, et al. Extracellular matrix remodeling and organization in developing and diseased aortic valves. *Circ. Res.* 98(11):1431–1438, 2006. https://doi.org/10.1161/01.RES.0000224114.65109.4e.



- ¹⁴Hinton, R. B., and K. E. Yutzey. Heart valve structure and function in development and disease. *Annu. Rev. Physiol.* 73:29–46, 2011.
- ¹⁵Hjortnaes, J., K. Shapero, C. Goettsch, J. D. Hutcheson, J. Keegan, J. Kluin, et al. Valvular interstitial cells suppress calcification of valvular endothelial cells. *Atherosclerosis*. 242(1):251–260, 2015. https://doi.org/10.1016/j.atherosclerosis.2015.07.008.
- ¹⁶Kanwar, A., J. J. Thaden, and V. T. Nkomo. Management of patients with aortic valve stenosis. *Mayo Clin. Proc.* 93(4):488–508, 2018. https://doi.org/10.1016/j.mayocp.201 8.01.020.
- ¹⁷Kloxin, A. M., J. A. Benton, and K. S. Anseth. In situ elasticity modulation with dynamic substrates to direct cell phenotype. *Biomaterials*. 31(1):1–8, 2010. https://doi.org/10.1016/j.biomaterials.2009.09.025.
- ¹⁸Kovacic, J. C., S. Dimmeler, R. P. Harvey, T. Finkel, E. Aikawa, G. Krenning, et al. Endothelial to mesenchymal transition in cardiovascular disease: JACC state-of-the-art review. *J. Am. Coll. Cardiol.* 73(2):190–209, 2019. https://doi.org/10.1016/j.jacc.2018.09.089.
- ¹⁹Landry, N. M., S. G. Rattan, and I. M. C. Dixon. an improved method of maintaining primary murine cardiac fibroblasts in two-dimensional cell culture. *Sci. Rep.* 9(1):12889, 2019. https://doi.org/10.1038/s41598-019-4928 5-9.
- ²⁰Livak, K. J., and T. D. Schmittgen. Analysis of relative gene expression data using real-time quantitative PCR and the 2(-Delta Delta C(T)) method. *Methods (San Diego, CA)*. 25(4):402–408, 2001. https://doi.org/10.1006/meth.20 01.1262.
- ²¹Mahler, G. J., E. J. Farrar, and J. T. Butcher. Inflammatory cytokines promote mesenchymal transformation in embryonic and adult valve endothelial cells. *Arterioscler. Thromb. Vasc. Biol.* 33:121–130, 2013. https://doi.org/10.1161/ATVBAHA.112.300504.
- ²²Markwald, R. R., T. P. Fitzharris, and F. J. Manasek. Structural development of endocardial cushions. *Am. J. Anat.* 148(1):85–119, 1977.
- ²³Markwald, R. R., T. P. Fitzharris, and W. N. Smith. Sturctural analysis of endocardial cytodifferentiation. *Dev. Biol.* 42(1):160–180, 1975.
- ²⁴Masters, K. S., D. N. Shah, G. Walker, L. A. Leinwand, and K. S. Anseth. Designing scaffolds for valvular interstitial cells: cell adhesion and function on naturally derived materials. *J. Biomed. Mater. Res. A.* 71(1):172–180, 2004. https://doi.org/10.1002/jbm.a.30149.
- ²⁵Mina, S., P. Huang, B. Murray, and G. Mahler. The role of shear stress and altered tissue properties on endothelial to mesenchymal transformation and tumor-endothelial cell interaction. *Biomicrofluidics*.11(4):044104, 2017. https://do i.org/10.1063/1.4991738.
- ²⁶Mina, S., W. Wang, Q. Qao, P. Huang, B. Murray, and G. Mahler. Shear stress magnitude and transforming growth factor-β1 regulate endothelial to mesenchymal transformation in a three-dimensional culture microfluidic device. *RSC Adv.* 6:85457–85467, 2016. https://doi.org/10.1039/C 6RA16607E.
- ²⁷O'Brien, K. D., D. D. Reichenbach, S. M. Marcovina, J. Kuusisto, C. E. Alpers, and C. M. Otto. Apolipoproteins B, (a), and E accumulate in the morphologically early lesion of 'degenerative' valvular aortic stenosis. *Arterioscler. Thromb. Vasc. Biol.* 16(4):523–532, 1996. https://doi.org/10.1161/01.atv.16.4.523.

- ²⁸O'Brien, K. D., C. M. Otto, D. D. Reichenbach, C. E. Alpers, and T. W. Wight. Regional accumulation of proteoglycans in lesions of "degenerative" valvular aortic stenosis and their relationship to apolipoproteins. *Circulation*. 92:612, 1995.
- ²⁹Puchtler, H., S. N. Meloan, and M. S. Terry. On the history and mechanism of alizarin and alizarin red S stains for calcium. *J. Histochem. Cytochem.* 17(2):110–124, 1969. h ttps://doi.org/10.1177/17.2.110.
- ³⁰Pudełko, A., G. Wisowski, K. Olczyk, and E. M. Koźma. The dual role of the glycosaminoglycan chondroitin-6-sulfate in the development, progression and metastasis of cancer. *FEBS J.* 286(10):1815–1837, 2019. https://doi.org/10.1111/febs.14748.
- ³¹Quinlan, A. M. T., and K. L. Billiar. Investigating the role of substrate stiffness in the persistence of valvular interstitial cell activation. *J. Biomed. Mater. Res. A.* 100A(9):2474–2482, 2012. https://doi.org/10.1002/jbm.a.34
- ³²Rabkin-Aikawa, E., M. Farber, M. Aikawa, and F. J. Schoen. Dynamic and reversible changes of interstitial cell phenotype during remodeling of cardiac valves. *J. Heart Valve Dis.* 13(5):841–847, 2004.
- ³³Richards, J., I. El-Hamamsy, S. Chen, Z. Sarang, P. Sarathchandra, M. H. Yacoub, et al. Side-specific endothelial-dependent regulation of aortic valve calcification: interplay of hemodynamics and nitric oxide signaling. *Am. J. Pathol.* 182(5):1922–1931, 2013. https://doi.org/10.1016/j.ajpath.2013.01.037.
- ³⁴Rodriguez, K. J., and K. S. Masters. Regulation of valvular interstitial cell calcification by components of the extracellular matrix. *J. Biomed. Mater. Res. A.* 90(4):1043–1053, 2009. https://doi.org/10.1002/jbm.a.32187.
- ³⁵Rutkovskiy, A., A. Malashicheva, G. Sullivan, M. Bogdanova, A. Kostareva, K. O. Stensløkken, et al. Valve interstitial cells: the key to understanding the pathophysiology of heart valve calcification. *J. Am. Heart Assoc.* 2017. https://doi.org/10.1161/jaha.117.006339.
- ³⁶Schneider, P. J., and J. D. Deck. Tissue and cell renewal in the natural aortic valve of rats: an autoradiographic study. *Cardiovasc. Res.* 15(4):181–189, 1981. https://doi.org/10.1 093/cvr/15.4.181.
- ³⁷Schneider, C. A., W. S. Rasband, and K. W. Eliceiri. NIH image to ImageJ: 25 years of image analysis. *Nat. Methods*. 9(7):671–675, 2012.
- ³⁸Sider, K. L., C. Zhu, A. V. Kwong, Z. Mirzaei, C. F. de Langé, and C. A. Simmons. Evaluation of a porcine model of early aortic valve sclerosis. *Cardiovasc. Pathol.* 23(5):289–297, 2014. https://doi.org/10.1016/j.carpath.201 4.05.004.
- ³⁹Stephens, E. H., J. G. Saltarrelli, L. S. Baggett, I. Nandi, J. J. Kuo, A. R. Davis, et al. Differential proteoglycan and hyaluronan distribution in calcified aortic valves. *Cardiovasc. Pathol.* 20(6):334–342, 2011. https://doi.org/10.1016/j.carpath.2010.10.002.
- ⁴⁰Taylor, P. M., P. Batten, N. J. Brand, P. S. Thomas, and M. H. Yacoub. The cardiac valve interstitial cell. *Int. J. Biochem. Cell Biol.* 35(2):113–118, 2003.
- ⁴¹Vesely, I. The role of elastin in aortic valve mechanics. *J. Biomech.* 31(2):115–123, 1998. https://doi.org/10.1016/s00 21-9290(97)00122-x.

Publisher's Note Springer Nature remains neutral with regard to jurisdictional claims in published maps and institutional affiliations.

